Quadrotor Trajectory Tracking Via SMC-Embedded Wild Horse Optimization

Thamer Al-Hsnawy*, Ali Al-Ghanimi

Department of Electrical Engineering, Faculty of Engineering, University of Kufa, Iraq, Najaf, Iraq

*Corresponding author E-mail: thamerm.alhsnawy@student.uokufa.edu.iq

Abstract. *This study provides an integrated control strategy with proportional derivative (PD) and sliding mode control (SMC) for a quadrotor. For inner loop control, the SMC, a robust nonlinear control method, is used to increase the system's resistance to uncertainty and shocks. By using high-speed switching in variable structure control, it reduces tracking mistakes. In the meantime, the PD control concentrates on tracking a helical path while controlling the outer loop for trajectory tracking. The PD and SMC parameters (k1, k2, and k3) could not be manually adjusted to produce acceptable results at first. As a result, this work presents an improvement by optimizing these control parameters using the Wild Horse Optimization (WHO) algorithm, a modern and cutting-edge optimization technique. This improvement shows good results in improving the quadrotor's tracking precision and stability, and it also greatly increases system performance. All simulations were performed in MATLAB, which facilitated detailed analysis and validation of the proposed control strategy.*

Keywords: Quadrotor, Optimization, PD, SMC, WHO.

1. INTRODUCTION

A flight vehicle commonly referred to as a drone or unmanned aerial vehicles (UAVs) in modern contexts, are airborne robots that have previously been connected with defense applications. UAVs can now be used for civilian tasks such as transporting medicines, packages, and other goods in containment zones in the COVID-19-affected area, establishing communication connections in disaster-stricken as, precision agriculture, and surveillance activities, thanks to advances in sensor technology and communication techniques. UAVs provide a plethora of chances to improve people's lives by assisting in the creation of Smart Cities. UAVs can be employed in future smart cities for data collecting, distant analysis, and speedy action execution [1] [2] [3] [4]. UAV are mainly divided into two classes: fixed-wing and rotating-blade aircraft as a quadrotor or a helicopter. fixed-wing are able to travel long distances spending much less energy that rotating-blade do, but contrary to fixed-wing, rotating-blade are able to perform hover flights. The development of convertible aircraft has been hampered by the complexity involved in the mechanical design [5]. A quadrotor UAV, also known as a quadcopter, is a type of rotary-wing drone characterized by its four rotors. The quadrotor design allows for vertical takeoff and landing (VTOL) capabilities, making it highly maneuverable and able to hover in place, which is not possible with traditional fixed-wing aircraft. Quadrotors are popular in various applications, including aerial photography, surveillance, and research, due to their ability to hover and perform agile maneuvers [6]. Control methods of the quadrotor can be categorized into linear and nonlinear control [7]. Common linear controls that received from researchers a

large interest are linear quadratic regulator (LQR), proportional integral derivative (PID), and H∞ control. Recently, multiple articles on nonlinear flight controllers for UAVs have been published. Among these, backstepping, feedback linearization, sliding mode control (SMC), active disturbance rejection rontrol (ADRC), and model predictive control have received much attention. The methods that involve adapting and estimating varying system parameters are known as adaptive controls. Adaptive control provides enhanced robustness in the presence of parametric uncertainties [8]. Also, there are intelligent controls for UAVs that involves the use of advanced algorithms and techniques to enhance the autonomy, adaptability, and decision-making capabilities of the UAV's control system [9]. Combines multiple control schemes to enhance the overall performance of a system refer as a hybrid controller. This approach often results in improved stability, robustness, and efficiency compared to using a single control scheme [10]. In this work, we focus on the implementation of first-order SMC for attitude control and PD control for position control. Recognizing that altitude control is relatively simple, we used only PD control in that section. To further refine this control approach, we incorporated the Wild Horse Algorithm (WHO) to optimize The PD and SMC parameters (k1, k2, and k3)

2. MATHEMATICAL MODEL

To develop a control system for the quadrotor, the first step is to derive the quadrotor mathematical model. Figure 1 displays the schematic diagram of the quadrotor, the derivation of the UAV dynamics involves two frames the earth frame E and the body frame B. The quadrotor is a complex system with nonlinearity. To simplify, the math modeling at the UAV, a few assumptions are adopted by[11].
Assumption 1: The body frame origin aligns with the center of mass of the quadrotor body.
Assumption 2: The UAV's interaction with the ground and any other surface is disregarded.
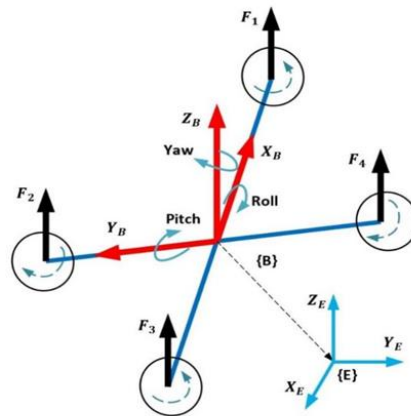
Fig. 1. The schematic diagram of the quadrotor

By applying these assumptions and information provided in the forgoing subsection on the quadrotor shown [13]. The dynamic model of the quadrotor may be obtained using the newton-euler approach, this model describes a six-degree of freedom (6 -DOF) to the x-type rigid body quadrotor , influenced by forces and moments is given as

$$\ddot{x} = \frac{U_1(\cos\phi\sin\theta\cos\psi + \sin\phi\sin\psi)}{m} \qquad (1)$$

$$\ddot{y} = \frac{U_1(sin\ \phi sin\ \theta cos\ \psi - cos\ \phi sin\ \psi)}{m} \tag{2}$$

$$\ddot{z} = \frac{U_1(cos\ \phi cos\ \theta)}{m} - g \tag{3}$$

$$\ddot{\phi} = \dot{\theta}\dot{\psi}\left(\frac{J_y - J_z}{J_x}\right) + \frac{l}{J_x}U_2 \tag{4}$$

$$\ddot{\theta} = \dot{\phi}\dot{\psi}\left(\frac{J_z - J_x}{J_y}\right) + \frac{l}{J_y}U_3 \tag{5}$$

$$\ddot{\psi} = \dot{\phi}\dot{\theta}\left(\frac{J_x - J_y}{J_z}\right) + \frac{l}{J_z}U_4 \tag{6}$$

the variables x,y,z represent the three locations of translational in the earth frame, while the pitching, rolling, and yawing movements are represented by the Euler angles ϕ, θ and ψ in radians. g is the gravitational acceleration. J_x, J_y and J_z are the moments of inertia of each axes measured by (kg.m). The variable m represents the mass of the quadrotor in kg, whereas J represent the inertia and l is the distance between the center of mass and the rotor of the quadrotor in meters. As an underactuated system, the quadrotor has four inputs that are applied to derive the 6-DOF. The input can be written as

$$U_1 = F_1 + F_2 + F_3 + F_4 \tag{7}$$

$$U_2 = F_3 - F_1 \tag{8}$$

$$U_3 = F_4 - F_2 \tag{9}$$

$$U_4 = F_1 + F_3 - F_2 - F_4 \tag{10}$$

the variables F_1, F_2, F_3 and F_4 represent the control forces produced by the propellers. U_1 the total thrust created by the UAV, which is the combined thrust of each rotor. Finally the roll torque is given by U_2 while the pitch torque is denoted by U_3. The yaw moment about the z-axis is represented by U_4 . Variations alter the yaw motion while maintaining constancy.

3. OPTIMIZATION ALGORITHM

Optimization constitutes a systematic approach aimed at enhancing a particular system's performance. It is an analytical process where in the most favorable configuration for a given problem is ascertained with the objective of optimizing a predefined criterion, typically encapsulated by a cost function. This procedure entails iterative experimentation with variations from an initial configuration, leveraging the accrued insights to navigate towards the global optimum

3.1. COST FUNCTION

In the domain of aeronautical control system optimization, the WHO algorithm stands as a metaphorically inspired method reflecting the collective behavior of equines for refining the parameters of a compound control PD and SMC in quadrotor applications. The algorithm operationalizes a cost function to critically appraise and discern the set of controller parameters that most effectively enhance the

quadrotor's flight stability, responsiveness, and energy consumption. This cost function typically encapsulates the variance between the quadrotor's actual trajectory and its targeted path, thereby quantifying the precision of flight control. The WHO algorithm iteratively evaluates various control configurations, analogized to a herd of horses, against the cost function, steering towards a configuration that yields the minimal value, indicative of optimal performance. Adopting metrics such as *integral of time-absolute error* aids in emphasizing both the magnitude and persistence of control errors, facilitating a more sophisticated PID tuning that promotes a harmonious balance between error correction and flight smoothness. The algorithm's iterative pursuit of minimization in the cost function's value mirrors the natural inclination of horses to seek the most favorable conditions, thus leading to an efficaciously tuned flight control system.

$$Integral\ Square\ Error\ (ISE) = \int_0^t (e(t))^2 dt \tag{11}$$

$$Integral\ Absolute\ Error\ (IAE) = \int_0^t |e(t)| dt \tag{12}$$

$$Integral\ Time\text{-}Square\ Error\ (ITSE) = t(e(t))^2 dt \tag{13}$$

$$Integral\ of\ Time\text{-}Absolute\ Error\ (ITAE) = \int_0^t t|e(t)| dt \tag{14}$$

where e(t) is the error signal in the time (t) domain.
The controller is used to reduce error signals, or, to minimize the value of the performance indices indicated above, in terms of error criteria. Because the smaller the value of the respective chromosomes' performance indices, the fitter the chromosomes will be, and vice versa, we define chromosomal fitness as:

$$fittnes\ value = \frac{1}{performance\ index} \tag{15}$$

3.2. WHO

The WHO algorithm offers a novel approach to address these challenges by emulating the natural behavior of wild horses in search of optimal grazing areas [12][13]. By leveraging the principles of leadership and follower dynamics within a herd, the WHO algorithm navigates the solution space dynamically, striking a balance between exploration and exploitation to converge towards globally optimal solutions [14]. In this thesis, we propose a novel methodology for tuning the control systems of quadrotor UAVs using the WHO algorithm. We focus on optimizing the parameters of PID controllers for balancing the quadrotor and improving performance metrics such as ascent time, settling time, overshoot, and error reduction. Additionally, we extend our study to incorporate dual-mode controllers, specifically SMC and PD controllers, for trajectory tracking tasks. The WHO algorithm's working mechanism can be summarized as follows:Problem Formulation: Define the control system parameters to be optimized, including PID gains for balancing and trajectory tracking tasks:

- Fitness Function Design: Develop a comprehensive cost function that quantifies the performance of the quadrotor based on specified metrics, such as ascent time, settling time, overshoot, and error reduction.
- WHO Algorithm Implementation: as shown in **fig. 2.** initialize a population of potential solutions (horses) representing different sets of control parameters. Employ the WHO algorithm to iteratively update the positions of horses based on their fitness values, mimicking the natural selection process.
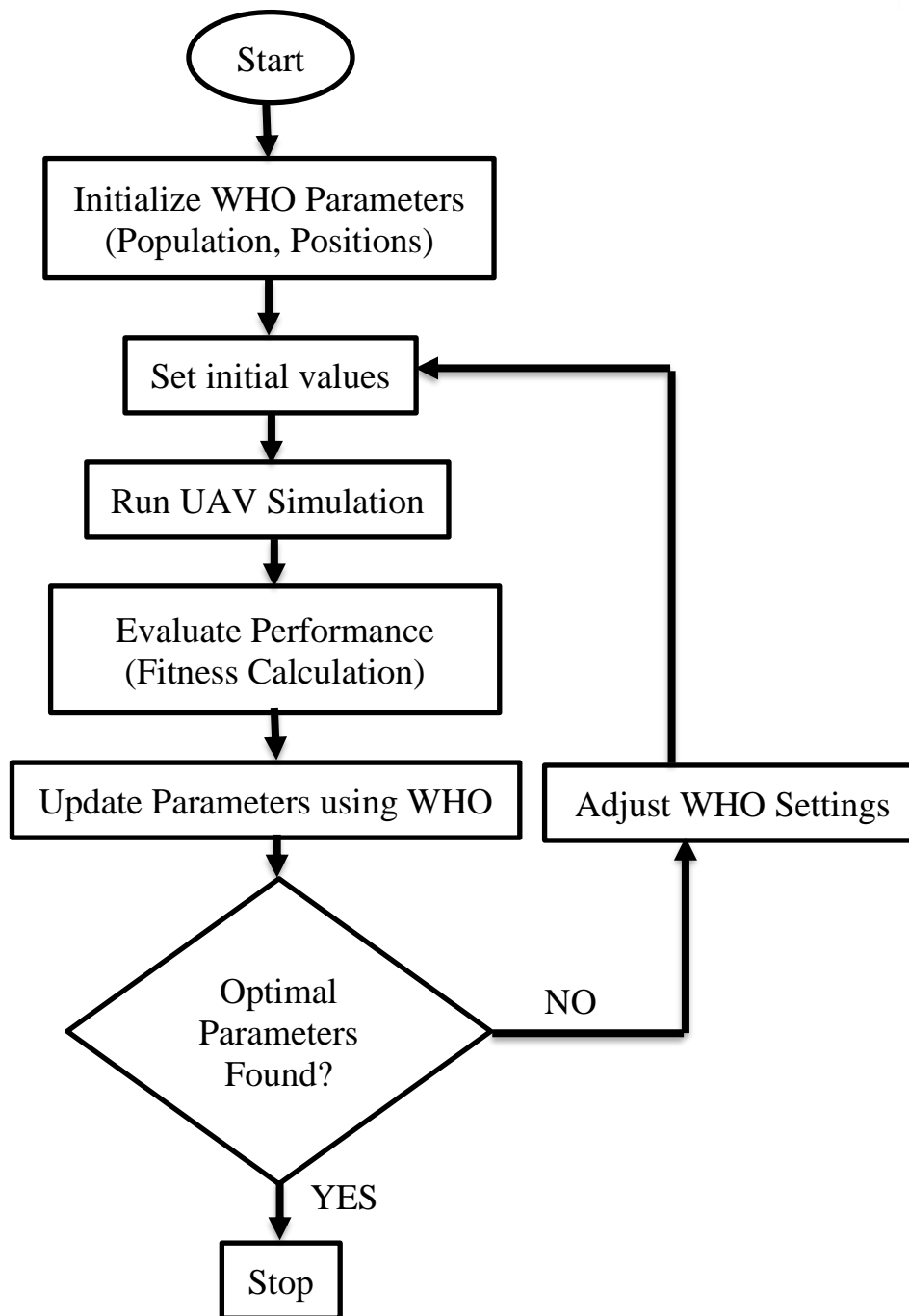
Fig. 2. Flowchart of WHO algorithm.

- Evaluation and Optimization: Assess the performance of each solution using the fitness function, and select leaders based on their fitness relative to the problem objectives. Update the herd dynamics to adapt and evolve towards optimal solutions, balancing exploration and exploitation.
- Validation and Analysis: Compare the performance of the optimized control systems obtained using the WHO algorithm with those obtained through traditional optimization methods. Evaluate the effectiveness of the WHO algorithm in improving the stability and maneuverability of quadrotor UAVs.

4. CONTROL METHOD

This section display the design and implementation of this control scheme, highlighting its effectiveness through simulation and real-world applications. **Fig. 3.** shows the Trajectory being tracked in 3D and with other perspectives. This particular screens shot is taken when the sliding mode control was used with the presence of wind.
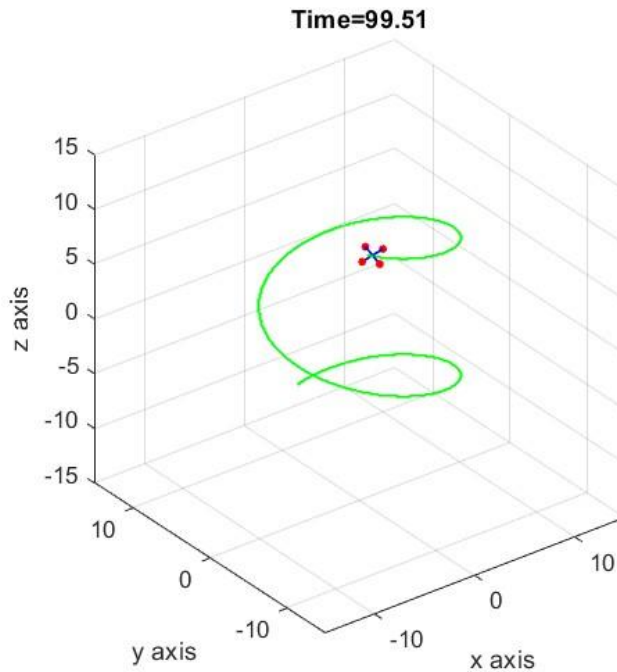
Fig. 3. The Helical trajectory.

For this purpose, the upcoming subsections will cover very general linear and non-linear control techniques design for quadrotor system. In linear control, the ubiquitous PD (Proportional Derivative) control has been studied, meanwhile the non-linear techniques the well-known conventional sliding mode control has been adopted. It should be noted that the attitude and the position control can be treated as separate modules. Thus, various permutations and combinations of independent control laws can be applied to position and attitude controlling task [15]. For instance, the position control can be done in PD control while attitude stabilization can be done using the SMC and vice versa. Unless otherwise mentioned, the generalized control block diagram for control of a quadrotor is shown in **fig. 4.**
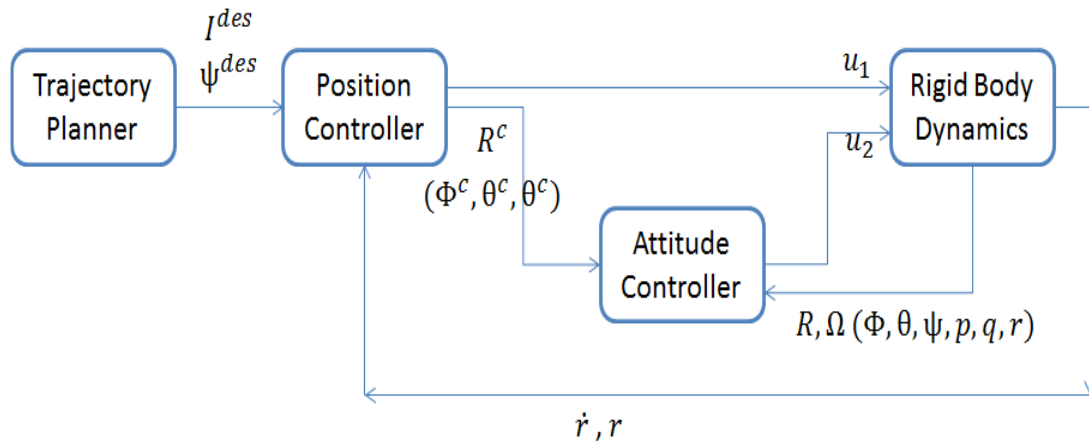
Fig. 4. General block diagram for control of a quadrotor.

The control trajectory tracking can be partitioned into two components. one that performs input/output linearization and another that aids in minimizing the tracking error. The initial order SMC is utilized in this context. In order to streamline the process, the sliding mode control is exclusively implemented in the attitude control section, while the PD control is employed for the position control section. The altitude control is straightforward and does not require complex control laws.

4.1. SMC

SMC is especially helpful in the case of quadrotors because of their intricate dynamics and requirement for exact control in order to maintain performance and stability. Because quadrotors are underactuated systems with nonlinear dynamics, traditional control techniques face several difficulties. SMC stands out as an appropriate control technique due to its resilience and capacity to manage such complications [16]. We used SMC to operate a quadrotor's inner loop while keeping the desired orientation (pitch, roll, and yaw) constant. We guaranteed the stability and responsiveness of the quadrotor by creating sliding surfaces for each of the Euler angles and obtaining suitable control laws. Pitch, roll, and yaw angle control laws were determined as follows.
Define the sliding surface for the angles:

$$s_\phi = \dot{e}_\phi + \lambda_\phi e_\phi \qquad (16)$$
$$s_\phi = \dot{e}_\phi + \lambda_\phi e_\phi \qquad (17)$$
$$s_\psi = \dot{e}_\psi + \lambda_\psi e_\psi \qquad (18)$$

where $\lambda_\phi, \lambda_\theta, \lambda_\psi$ are positive constants and e_ϕ, e_θ and e_ψ are the error signal to the three SMCs ϕ, θ, and ψ respectively and they are the difference between the desired and the actual signals as follows:

$$e_\phi = \phi_{des} - \phi_{act} \qquad (19)$$
$$e_\theta = \theta_{des} - \theta_{act} \qquad (20)$$
$$e_\psi = \psi_{des} - \psi_{act} \qquad (21)$$

Control Law for roll angel (ϕ)

To derive the control law, we start with the sliding surface dynamics:

$$\dot{s}_\phi = \ddot{e}_\phi + \lambda_\phi \dot{e}_\phi \tag{22}$$

$$\dot{s}_\phi = (\ddot{\phi}_{des} - \ddot{\phi}_{act}) + \lambda_\phi(\dot{\phi}_{des} - \dot{\phi}_{act}) \tag{23}$$

substituting the expressions for $\ddot{\phi}_{act} = \ddot{\phi}$ given by equations (4) and $\ddot{\phi}_{des}$

$$\dot{s}_\phi = \ddot{\phi}_{des} - \left(\dot{\psi}\theta\left(\frac{J_y - J_2}{J_x}\right) + \frac{l}{J_x}U_2\right) + \lambda_\phi(\dot{\phi}_{des} - \dot{\phi}_{act}) \tag{24}$$

Solving for U_2 :

$$U_2 = \frac{J_x}{l}\left(\dot{\psi}\theta\left(\frac{J_y - J_x}{J_x}\right) - \ddot{\phi}_{des} + \lambda_\phi(\dot{\phi}_{act} - \dot{\phi}_{des})\right) \tag{25}$$

Control Law for Pitch Control ($\boldsymbol{\theta}$)
To derive the control law, we start with the sliding surface dynamics:

$$\dot{s}_\theta = \ddot{e}_\theta + \lambda_\theta \dot{e}_\theta \tag{26}$$

$$\dot{s}_\theta = (\ddot{\theta}_{des} - \ddot{\theta}_{act}) + \lambda_\theta(\dot{\theta}_{des} - \ddot{\theta}_{act}) \tag{27}$$

Substituting the expressions for $\ddot{\theta}_{act} = \ddot{\theta}$ given by equations (5) and $\ddot{\theta}_{des}$

$$\dot{s}_\theta = -\left(\dot{\phi}\dot{\psi}\left(\frac{J_z - J_x}{J_y}\right) + \frac{l}{J_y}U_3\right) + \lambda_\theta(\dot{\theta}_{des} - \dot{\theta}_{act}) \tag{28}$$

Solving for U_3 :

$$U_3 = \frac{J_y}{l}\left(\dot{\phi}y\left(\frac{J_x - J_x}{J_y}\right) - \ddot{\theta}_{des} + \lambda_\theta(\dot{\theta}_{act} - \dot{\theta}_{des})\right) \tag{29}$$

Control Law for Yaw Control ($\boldsymbol{\psi}$)
To derive the control law, we start with the sliding surface dynamics:

$$\dot{s}_\psi = \ddot{e}_\psi + \lambda_\psi \dot{e}_\psi \tag{30}$$

$$\dot{s}_\psi = (\ddot{\psi}_{des} - \ddot{\psi}_{act}) + \lambda_\psi(\dot{\psi}_{des} - \dot{\psi}_{act}) \tag{31}$$

Substituting the expressions for $\ddot{\psi}_{act} = \ddot{\psi}$ given by equations (6) and $\ddot{\psi}_{des} = \dot{\psi}_{des} = 0$

$$\dot{s}_\psi = -\left(\dot{\theta}\dot{\phi}\left(\frac{J_x - J_y}{J_z}\right) + \frac{l}{J_z}U_4\right) - \lambda_\psi(\dot{\psi}_{act}) \tag{32}$$

Solving for U$_3$:

$$U_4 = \frac{J_z}{l}\left(\dot{\theta}\dot{\phi}\left(\frac{J_x - J_y}{J_z}\right) + \lambda_\psi(\dot{\psi}_{act})\right) \tag{33}$$

Switching Control and Stability Analysis

Incorporating the switching control term:

$$U_{sw} = -k_i sgn\ (s_i),\ k_i > 0 \tag{34}$$

$$U_T = U_i + U_{sw} \tag{35}$$

Using the Lyapunov function to analyze stability:

$$V_i = \frac{1}{2}s_i^2 \tag{36}$$

$$\dot{V}_i = s_i \dot{s}_i = -k_i |s_i| \tag{37}$$

Since $\dot{V}_i$ is negative definite, the system is stable.

4.2. PD

PD control is a fundamental linear control strategy known for its simplicity and computational efficiency [17]. It can be easily implemented in real-time systems using microcontrollers. Its straightforward mathematical formulation and ease of comprehension contribute to its widespread application in aerial robotics. For controlling the position of the quadrotor in the x,y, and y directions, we use PD controllers. The PD control design for position (outer loop) is expressed as :

$$U_x = K_{px}(x_{des} - x) + K_{dx}(\dot{x}_{des} - \dot{x}) \tag{38}$$

$$U_y = K_{py}(y_{des} - y) + K_{dy}(\dot{y}_{des} - \dot{y}) \tag{39}$$

$$U_z = K_{pz}(z_{des} - z) + K_{dz}(\dot{z}_{des} - \dot{z}) \tag{40}$$

where,

- U_x, U_y, U_z are the control inputs for the position.
- $x_{des}, y_{des}, z_{des}$ are the desired positions.
- K_{px}, K_{py}, K_{pz} are the proportional gains.
- K_{dx}, K_{dy}, K_{dz} are the derivative gains.

These control inputs are then converted into desired angles for the inner loop:

$$\phi_{des} = \frac{1}{g}\left(U_x sin\ \psi - U_y cos\ \psi\right) \tag{41}$$

$$\theta_{des} = \frac{1}{g}\left(U_x cos\ \psi + U_y sin\ \psi\right) \tag{42}$$

$$\psi_{des} = \psi_{des}\ (predefined\ or\ kept\ constant). \tag{43}$$

5.SIMULATION PARAMETERS SETTING

This section will present the predetermined and variable parameters pertaining to the quadrotor model and the optimization procedures.

5.1.Model Parameters

The DJI F450 has a mass of 964 g and an arm length of 22 cm. The quadrotor's physical specifications can be found in Table (1).

Table (1): Model parameters, taken from real quadcopter system datasheets and experiment (DJI F-450 frame)

Description	Variable symbol	Value	Unit
Total mass of quadrotor	m	0.964	kg
Distance form center of quadrotor to the motor	l	0.22	m
Quadrotor moment of inertia around X axes	J_x	8.55×10^{-3}	$kg.m^2$
Quadrotor moment of inertia around Y axes	J_y	8.55×10^{-3}	$kg.m^2$
Quadrotor moment of inertia around Z axes	J_z	1.48×10^{-3}	$kg.m^2$
Rotational moment of inertia around the ropeller axis	J_r	5.225×10^{-5}	$kg.m^2$
Gravitational acceleration	g	9.81	m/s^2

5.2. WHO PARAMETERS

Table (4.3) displays the parameters specified to the WHO used in this work.

Table (2): The WHO parameters For Balancing and Trajectory Tracking

Description	Parameter	Value/ WHO
Population Size	N	60
Maximum Iterations	Max_iter	100
Lower Bound	lb	0
Upper Bound	ub	100
Dimension	dim	9
Stallion Percentage	ps	0.2
Crossover Percentage	pc	0.13
Stallion Exchange Rate	SER	0.2

6. Results

The fig. (5-7) show the results. Before optimization, the control system used a PD controller for the outer ring and a sliding position control for the inner ring. While it has demonstrated robustness to disturbances, such as wind, it has exhibited large deflections and a long period of stability. As a result, a WHO algorithm was developed to enhance system robustness and response time by optimizing control settings. Post-optimization results showed a noticeable improvement: the system achieved faster stabilization, reduced oversteer, and efficiently maintained adherence to the target path even in the presence of external disturbances. The comparison demonstrates the effectiveness of the WHO algorithm in optimizing control tactics to obtain superior performance in dynamic conditions.
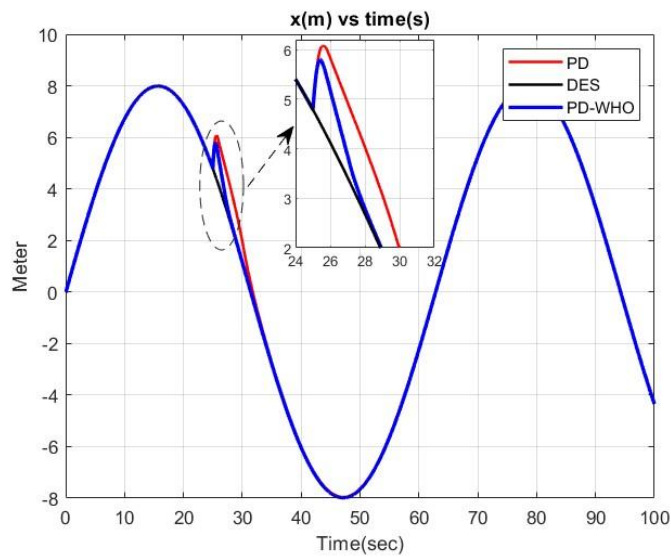
Fig. 5. x-axis tracking versus time [with disturbance at 25 seconds]
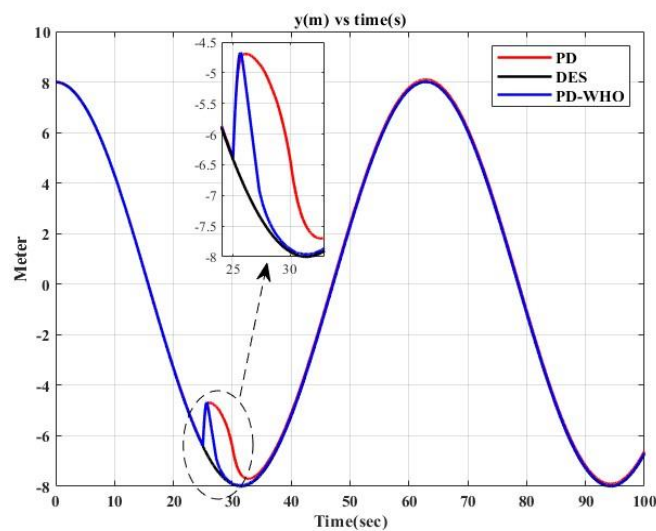
Fig. 6. y-axis tracking versus time [with disturbance at 25 seconds]
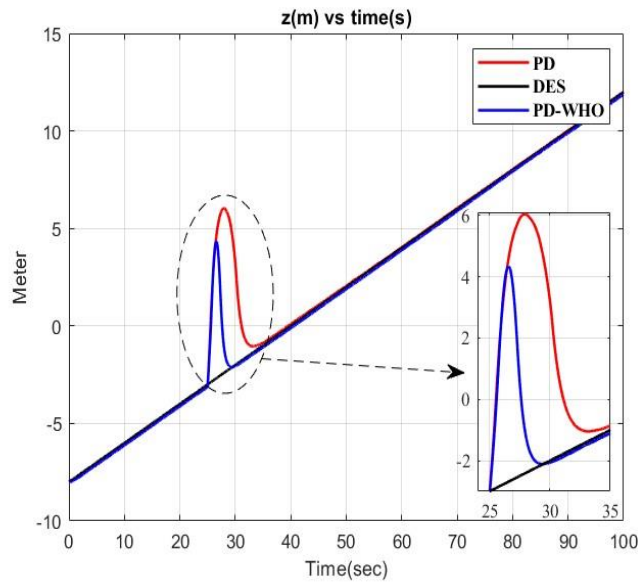
Fig. 7. x-axis tracking versus time [with disturbance at 25 seconds]

The results demonstrate in the fig. (8-9) the effectiveness of a control system employing standard SMC and an improved version with WHO. The focus is on the pitch and roll response, specifically when a substantial disturbance is introduced at 25 seconds. Both control systems initially exhibit accurate tracking of their desired values. However, when a disturbance occurs, the standard sliding mode control SMC method demonstrates a significant divergence in both pitch and roll, accompanied by a pronounced oscillation in pitch. On the other hand, the WHO-enhanced SMC rapidly achieves stability, closely following the intended paths and showing better performance by effectively correcting deviations and maintaining a smoother, more consistent response for the rest of the testing duration.
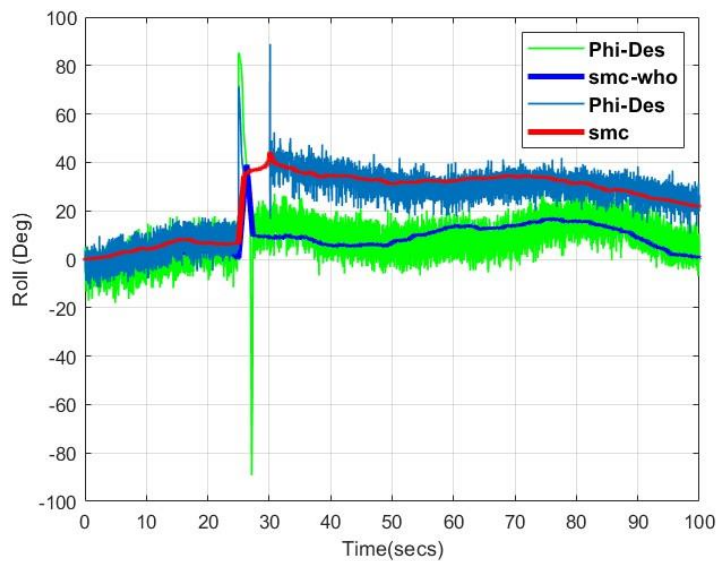
Fig. 8. phi angle tracking versus time [with disturbance at 25 seconds]
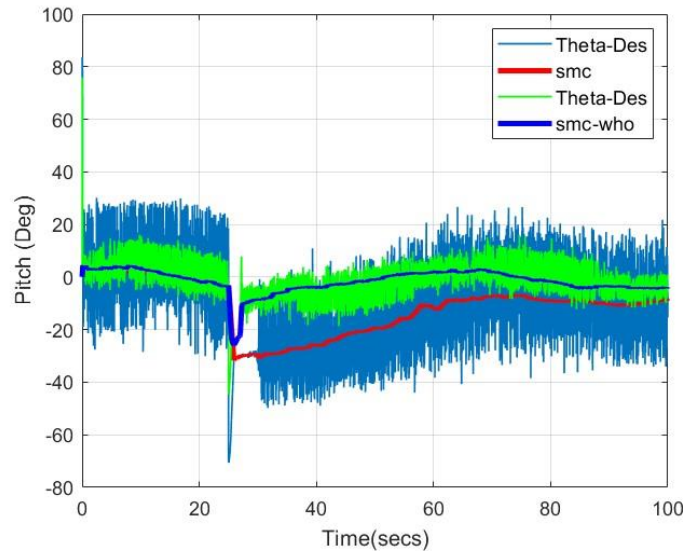
Fig. 9. theta tracking versus time with disturbance at 25 seconds]

The fig. (10) displays the yaw angle responses of a control system employing normal SMC and an optimised version with WHO. These responses are contrasted to a target yaw trajectory of zero degrees. The conventional SMC initially aligns with the target but exhibits considerable susceptibility to disturbances introduced at approximately the 25-second mark, deviating substantially from the ideal angle. On the other hand, the WHO-enhanced SMC shows better performance by swiftly readjusting to the target path after a disruption and maintaining a closer adherence. This is especially seen in the fast stabilisation and reduced deviations between 25 to 32 seconds. This demonstrates the efficacy of WHO in improving the accuracy and adaptability of control measures in response to abrupt shifts in the environment.
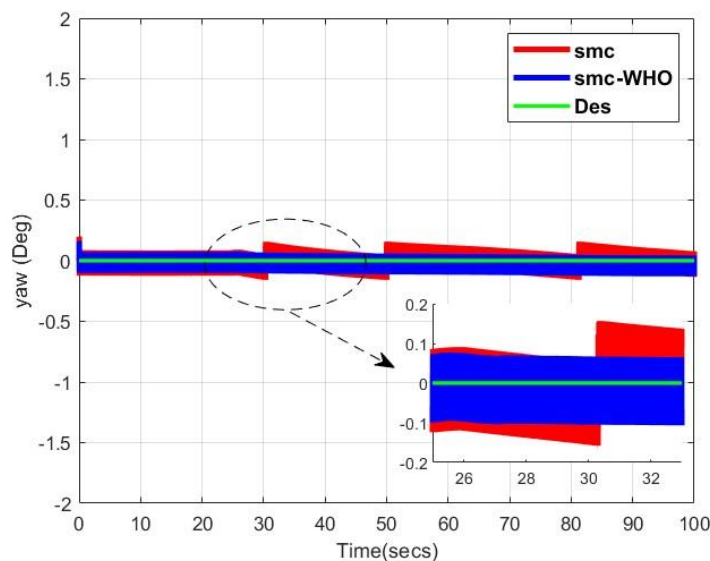
Fig. 10. yaw tracking versus time with disturbance at 25 seconds]

The fig. (11-14) representing control inputs U1, U2, U3, and U4 demonstrate different reactions to a disturbance introduced around the 25-second mark. Each graph represents a distinct facet of the control strategy's efficacy in reducing the influence of the disturbance. Together, these control inputs showcase the system's capacity to adjust and maintain stability after disruptions, with different levels of control exertion and accuracy. Every input makes a distinct contribution to the overall stability of the system, demonstrating a well-coordinated control technique that efficiently reduces disturbances and maintains uninterrupted operation.
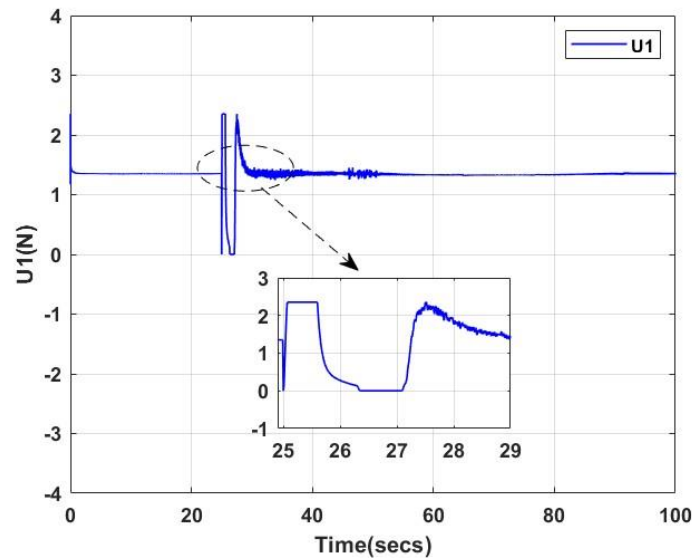
Fig. 11. Thrust Inputs vs Time [with disturbance at 25 seconds]
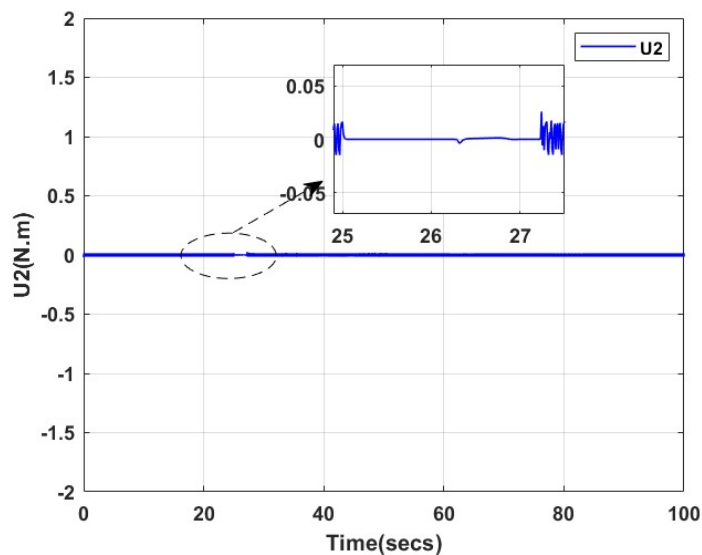
Fig. 12. Rolling Inputs vs Time [with disturbance at 25 seconds]
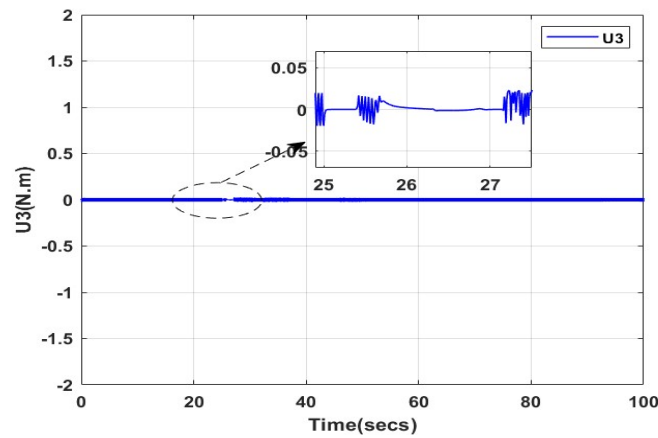
Fig.13. Pitching Inputs vs Time [with disturbance at 25 seconds]
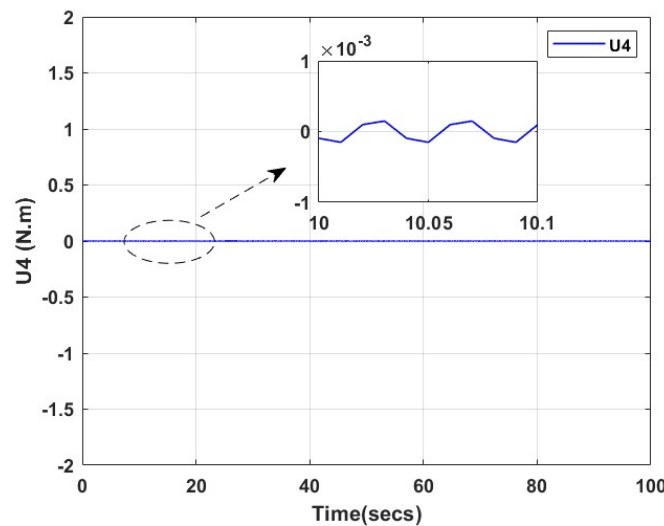
Fig. 14. Yawing Inputs vs Time [with disturbance at 25 seconds]

The fig. (15-17) demonstrate the efficacy of the WHO algorithm in improving the error management capabilities of a control system that employs . The WHO-enhanced SMC regularly outperforms the normal SMC by recovering faster and retaining significantly lower error levels in the x, y, and z coordinates once a disturbance is introduced at the 25-second point. This optimisation greatly decreases sudden increases in errors and enhances the stability of the system more effectively, emphasising the function of the WHO algorithm in fine-tuning the control parameters to guarantee strong and accurate control even under unfavourable conditions. The enhanced error management is essential for applications that require exceptional accuracy and dependability, highlighting the tangible advantages of incorporating modern optimisation approaches into control systems.
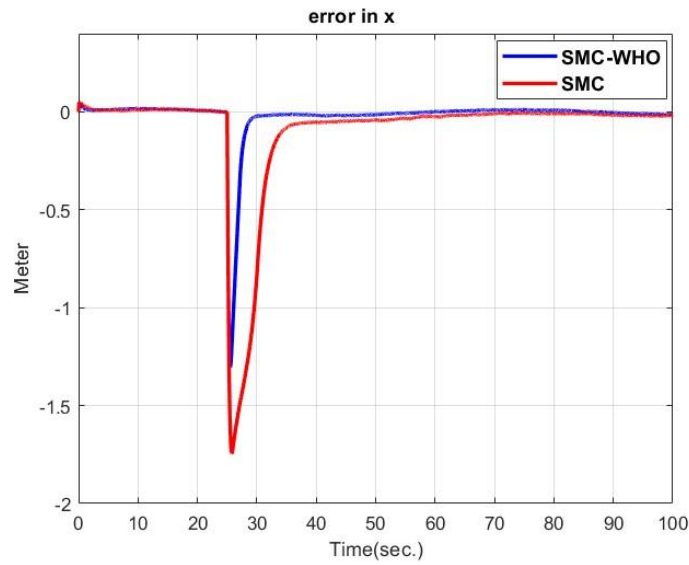
Fig. 15. Errors in x [with disturbance at 25 seconds]
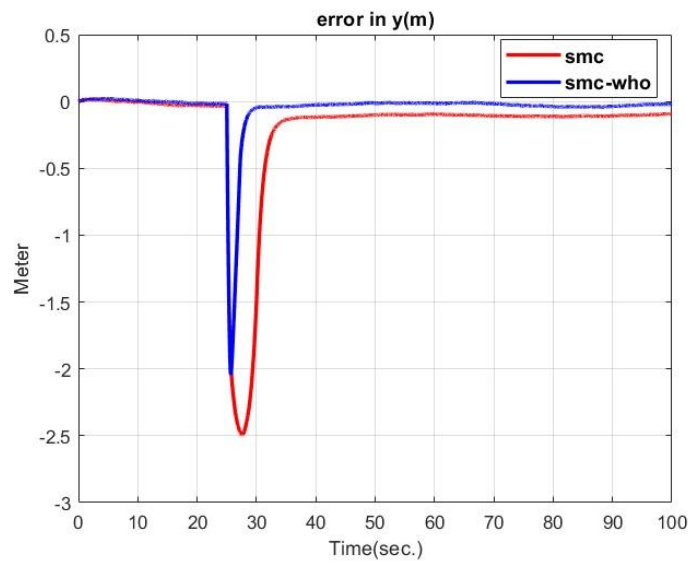
Fig. 16. Errors in y [with disturbance at 25 seconds]
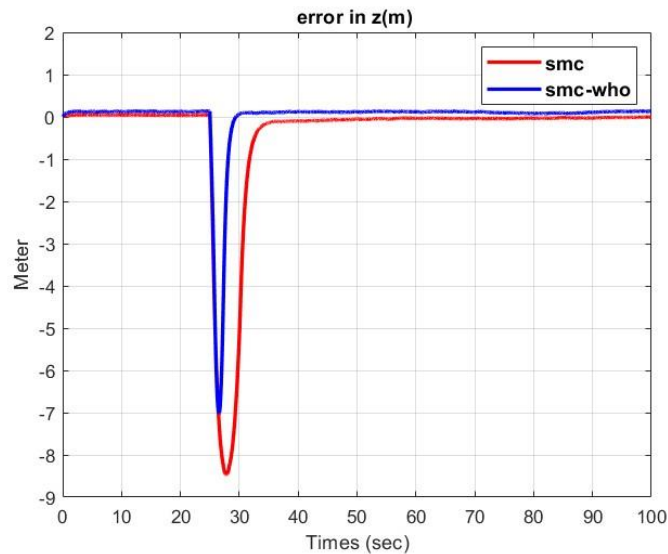
Fig. 17. Errors in z [with disturbance at 25 seconds]

7. CONCLUSION

This study investigates the improvement of control systems for quadcopters by utilizing modern control techniques and optimization algorithms. It focuses on dealing with the dynamic and unstable characteristics of these UAVs. The main discoveries consist of the creation of a unique control technique that integrates SMC for the internal loop with PD control for the external loop. This combination greatly enhances the accuracy of following a desired direction and reduces any deviations, especially when navigating intricate spiral patterns. In addition, the WHO method was employed to tune the parameters of both SMC and PD controllers, resulting in significant enhancements in response times and trajectory accuracy, while significantly reducing error margins. These advancements not only improve quadcopter management but also expand the use of UAVs in important fields such as emergency response, environmental monitoring, and urban planning. The work showcases the efficacy of combining complex optimization algorithms with robust control systems to address the difficulties in operating quadcopters. The successful implementation of the WHO algorithm represents a noteworthy progress in the field of UAV technology research and development.

REFERENCES

[1]   A. Utsav, A. Abhishek, P. Suraj, and R. K. Badhai, "An IoT based UAV network for military applications," in 2021 Sixth International Conference on Wireless Communications, Signal Processing and Networking (WiSPNET), IEEE, 2021, pp. 122–125.

[2]   G. E. Jeler, "Military and civilian applications of UAV systems," in INTERNATIONAL SCIENTIFIC CONFERENCE STRATEGIES XXI. The Complex and Dynamic Nature of the Security Environment-Volume 1, Carol I National Defence University Publishing House, 2019, pp. 379–386.

[3] S. A. H. Mohsan, M. A. Khan, F. Noor, I. Ullah, and M. H. Alsharif, "Towards the unmanned aerial vehicles (UAVs): A comprehensive review," Drones, vol. 6, no. 6, p. 147, 2022.

[4] S. K. Chaturvedi, R. Sekhar, S. Banerjee, and H. Kamal, "Comparative review study of military and civilian unmanned aerial vehicles (UAVs)," INCAS Bull., vol. 11, no. 3, pp. 181–182, 2019.

[5] J. A. Bautista-Medina, R. Lozano, and A. Osorio-Cordero, "Modeling and control of a single rotor composed of two fixed wing airplanes," Drones, vol. 5, no. 3, pp. 1–18, 2021, doi: 10.3390/drones5030092.

[6] S. I. Abdelmaksoud, M. Mailah, and A. M. Abdallah, "Control strategies and novel techniques for autonomous rotorcraft unmanned aerial vehicles: A review," IEEE Access, vol. 8, pp. 195142–195169, 2020.

[7] Y. M. Al-Younes, M. A. Al-Jarrah, and A. A. Jhemi, "Linear vs. nonlinear control techniques for a quadrotor vehicle," in 7th International Symposium on Mechatronics and its Applications, IEEE, 2010, pp. 1–10.

[8] H. Mo and G. Farid, "Nonlinear and adaptive intelligent control techniques for quadrotor uav–a survey," Asian J. Control, vol. 21, no. 2, pp. 989–1008, 2019.

[9] T. Yüksel, "An intelligent visual servo control system for quadrotors," Trans. Inst. Meas. Control, vol. 41, no. 1, pp. 3–13, 2019.

[10] A. Khalid, Z. Mushtaq, S. Arif, K. Zeb, M. A. Khan, and S. Bakshi, "Control schemes for quadrotor UAV: taxonomy and survey," ACM Comput. Surv., vol. 56, no. 5, pp. 1–32, 2023.

[11] T. O. Olayinka, A. A. Olatide, A. D. Oluwagbemiga, and M. O. Okelola, "Internal model control tuned proportional integral derivative for quadrotor unmanned aerial vehicle dynamic model," Control. Theory Inform.(IISTE), vol. 9, pp. 1–10, 2020.

[12] R. Sharifi and M. Ramezanpour, "Customer Behavior Analysis using Wild Horse Optimization Algorithm," *Majlesi J. Telecommun. Devices*, vol. 12, no. 2, pp. 79–93, 2023, doi: 10.30486/MJTD.2023.1980070.1025.

[13] R. Sharifi and M. Ramezanpour, "An Improved Decision Tree Classification Method based on Wild Horse Optimization Algorithm," *Majlesi J. Telecommun. Devices*, vol. 12, no. 4, pp. 177–188, 2023, doi: 10.30486/mjtd.2023.1980072.1026.

[14] Y. Li, Q. Yuan, M. Han, and R. Cui, "Hybrid Multi-Strategy Improved Wild Horse Optimizer," *Adv. Intell. Syst.*, vol. 4, no. 10, 2022, doi: 10.1002/aisy.202200097.

[15] M. Schwung, D. Vey, and J. Lunze, "Quadrotor Tracking Control: Design and Experiments," *CCTA 2019 - 3rd IEEE Conf. Control Technol. Appl.*, pp. 768–775, 2019, doi: 10.1109/CCTA.2019.8920572.

[16] J. Liu, *Sliding mode control using MATLAB*. 2017.

[17] A. Kherkhar, F. Didi, and Y. Chiba, "Proportional Derivative (PD) -Based Interval Type-2 Fuzzy Control Design of a Quadrotor Unmanned Aerial Vehicle," *Tob. Regul. Sci.*, vol. 9, no. 1, pp. 3419–3440.